Simulation Of Mechanical Systems With Multiple Frictional Contacts

MS-CIS-92-16
GRASP LAB 303

Yin-Tien Wang
Vijay Kumar

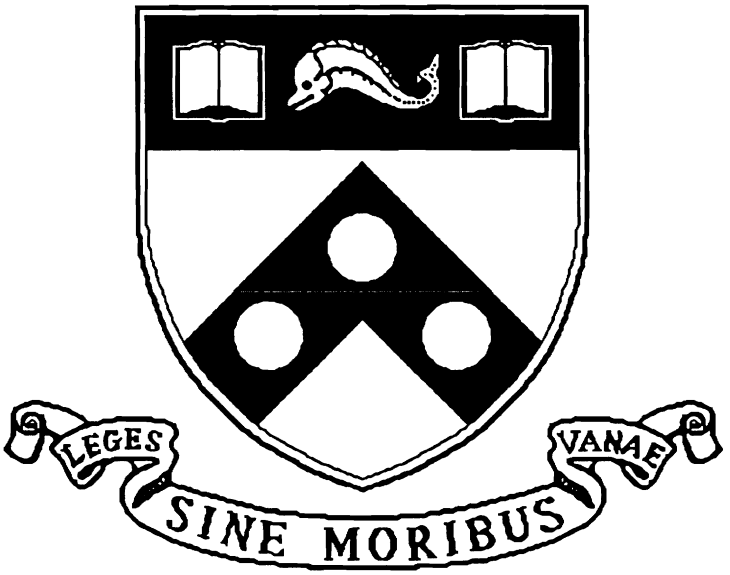

University of Pennsylvania
School of Engineering and Applied Science
Computer and Information Science Department
Philadelphia, PA 19104-6389

March 1992

SIMULATION OF MECHANICAL SYSTEMS WITH MULTIPLE FRICTIONAL CONTACTS

Yin-Tien Wang
Research Assistant
yintien@grip.cis.upenn.edu

Vijay Kumar
Assistant Professor
kumar@central.cis.upenn.edu

Department of Mechanical Engineering and Applied Mechanics
University of Pennsylvania, Philadelphia, PA

Abstract

There are several applications in robotics and manufacturing in which nominally rigid objects are subject to multiple frictional contacts with other objects. In most previous work, rigid body models have been used to analyze such systems. There are two fundamental problems with such an approach. Firstly, the use of frictional laws, such as Coulomb's law, introduce inconsistencies and ambiguities when used in conjunction with the principles of rigid body dynamics. Secondly, hypotheses traditionally used to model frictional impacts can lead to solutions which violate principles of energy conservation. In this paper these problems are explained with the help of examples. A new approach to the simulation of mechanical systems with multiple, frictional constraints is proposed which is free of inconsistencies.

1 Introduction

1.1 Background

In many high speed processes involving manufacturing equipment or robots several bodies will undergo multiple, concurrent, dynamic frictional contacts. Examples in an industrial setting arise in part feeding systems where a component is fed, typically at high speeds, along guides or rollers, and in the process, experiences multiple impacts with surrounding rigid bodies before arriving at its final destination. It is important to determine the orientation and position of the component at the final position and to optimize the process with respect to predetermined objectives. In automatic assembly of mechanical components [1-3,23,39], for example, the insertion of a peg into a hole, there are several configurations in which the peg can contact the hole or the slot [73]. If this operation must be performed rapidly, it is of interest to predict the behavior of the system under different operating conditions for all possible configurations. In robot systems such as multifingered grippers,

multi-arm systems, or multi-legged walking vehicles, several limbs are used to constrain and manipulate an object [11,38,62,78]. In all these examples the occurrence of multiple, frictional contacts complicates the dynamic analysis and the simulation (the prediction of motion given the external forces and moments on the system).

1.2 Previous work

There is an extensive literature on analytical methods for dynamic simulation of mechanical systems, automatic generation of the equations of motion for complex mechanisms and computer aided methods for analysis [15,24,25,40,53,66,72]. In most of these works, the emphasis is on the dynamics of mechanical linkages which, for the most part, are characterized by bilateral, holonomic constraints [35,60].

There is much less literature about systems in which there are multiple contacts between rigid bodies. The constraints that are arise in such situations are called unilateral constraints [35,74] because the contact forces (and relative displacements) can be defined so that they are non-negative. The contacts are intermittent - an active constraint can become passive or inactive, while an inactive constraint can become active. Such an event changes the behavior of the system - the number of kinematic constraints and therefore, the number of degrees of freedom of the system is changed, the dimension of the constraint manifold is different and the governing system of differential equations changes. Hence, we use the term *changing topology* [19] to capture the essence of such systems.

In the event of a passive constraint becoming active, the change is generally accompanied by an impact which is characterized by impulsive forces. The first systematic study of impact between two bodies with friction dates back to Routh's work [61] in 1891. Since his treatise, very little has been done in terms of understanding rigid body impacts with friction. More recently, the emphasis on computer oriented approaches to analysis and dynamic simulation of systems (including systems with impacts) [24,75,76] rekindled the interest in mechanical systems with unilateral constraints [8,34,71]. Featherstone [16], Lötstedt [42] and Mason and Wang [47] pointed out some of the inconsistencies which arise when rigid body models are used with Coulomb's empirical law of friction [60]. For example, if we consider the simulation of a rod sliding along a rough ground in a plane with a single contact, there are configurations in which no solutions (that are consistent with the constraints) exist[1], and others in which the solution is not unique. Duvaut and Lions explored the existence and uniqueness issues with deformable bodies in static contact [14].

---

[1]This is explained with the help of an example in Section 3.3.

Because of the complexity encountered in the dynamic simulation of systems with multiple contacts, there has been considerable interest in quasi-static simulations wherever it can be justified. A quasi-static simulation of the "peg in the hole" operation in order to study the effect of remote center compliance is presented in [74] and formulation of the minimum power principle for quasi-static simulation is described in [56]. Similar studies can also be found in robot grasping [11,62], motion planning [12,27] and pushing operations [46]. Screw system theory has facilitated the modeling of multiple spatial constraints for the quasi-static analysis of assembly operations [51,70] and robotic grasps [36,37,62].

Computer simulation of mechanical systems has generated considerable interest in the computer graphics community. For the most part, the emphasis has been on realistic graphical displays rather than on accurate simulation of the behavior of the system. For example, see References [4,5,58].

1.3 Organization

In this paper, two key problem areas in the dynamics of rigid bodies with multiple frictional contacts are solved. First, the modeling of rigid body collisions is addressed. Second, an accurate model that will predict the contact forces (normal and frictional) is sought. The emphasis here is on correct phenomenological and quantitative modeling. In the next section, we describe existing impact models and some of the difficulties that may arise when they are used. In Section 3, we address the problem of determining contact forces (in the absence of impacts) and demonstrate that the use of Coulomb's frictional law with the rigid body assumption may result in inconsistencies or ambiguities. Next, our dynamic model of mechanical systems is described in which the compliance at each contact is incorporated. This approach is attractive because it is free of inconsistencies and because any material property can be incorporated into the model. We illustrate this with the help of a simple example.

2 Rigid Body Collisions

2.1 Introduction

When two objects collide with one contact as shown in Figure 1, the principle of impulse and momentum provides the following relations:

$$M_1(\bar{v}_{1x} - \bar{V}_{1x}) = P_x \tag{2.1a}$$

$$M_1(\bar{v}_{1y} - \bar{V}_{1y}) = P_y \tag{2.1b}$$

$$I_1(\omega_1 - \Omega_1) = r_{1y}P_x - r_{1x}P_y \tag{2.1c}$$

$$M_2(\bar{v}_{2x} - \bar{V}_{2x}) = - P_x \tag{2.1d}$$

$$M_2(\bar{v}_{2y} - \bar{V}_{2y}) = - P_y \tag{2.1e}$$

$$I_2(\omega_2 - \Omega_2) = r_{2x}P_y - r_{2y}P_x \tag{2.1f}$$

where $\bar{V}$ and $\bar{v}$ are the initial and terminal velocities of mass center, respectively. Similarly, Ω and ω are initial and terminal angular velocities of mass center, $P_y(t)$ and $P_x(t)$ are the normal and tangential impulses. r_1 and r_2 are as shown in the figure, and M_1, M_2, I_1 and I_2 are the masses and moments of inertia for the two bodies.. There are six equations and eight unknowns (six velocity components and two impulses).

Two more equations are required in order to solve this problem. One equation is obtained from the friction model. For example, using Coulomb's law of friction, according to Routh [61], the tangential impulse is related to the normal impulse by

$$\frac{|dP_x|}{dP_y} \leq \mu \tag{2.2}$$

If sticking occurs, the relative velocity at the point of contact is zero and if the two bodies slide over one another, the equality in (2.2) holds. Now we have seven equations in the eight unknowns. The indeterminacy is resolved by hypothesizing a model for the impact. Several impact hypotheses for rigid body collisions are discussed in Section 2.3.

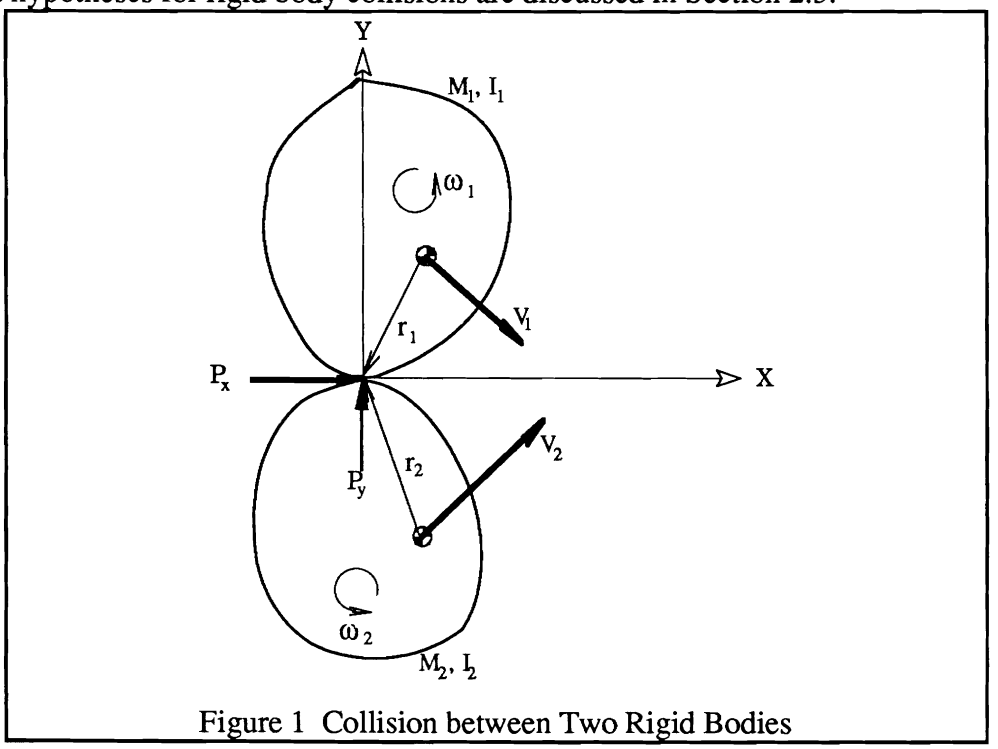

Figure 1 Collision between Two Rigid Bodies

2.2 The velocity-impulse diagram

Consider the collision between two rigid bodies. With all possible values of normal impulse, P_y, relative sliding and compressive velocities, S and C, there are five possible cases of impact [23,71]. They are (a) sliding and reverse sliding in compression phase; (b) sliding and reversed sliding in restitution phase; (c) sliding and sticking in compression phase; (d) sliding and sticking in restitution phase; and (e) forward sliding. Here $S = v_{1x} - v_{2x}$ and $C = v_{1y} - v_{2y}$ as shown in Figure 1.

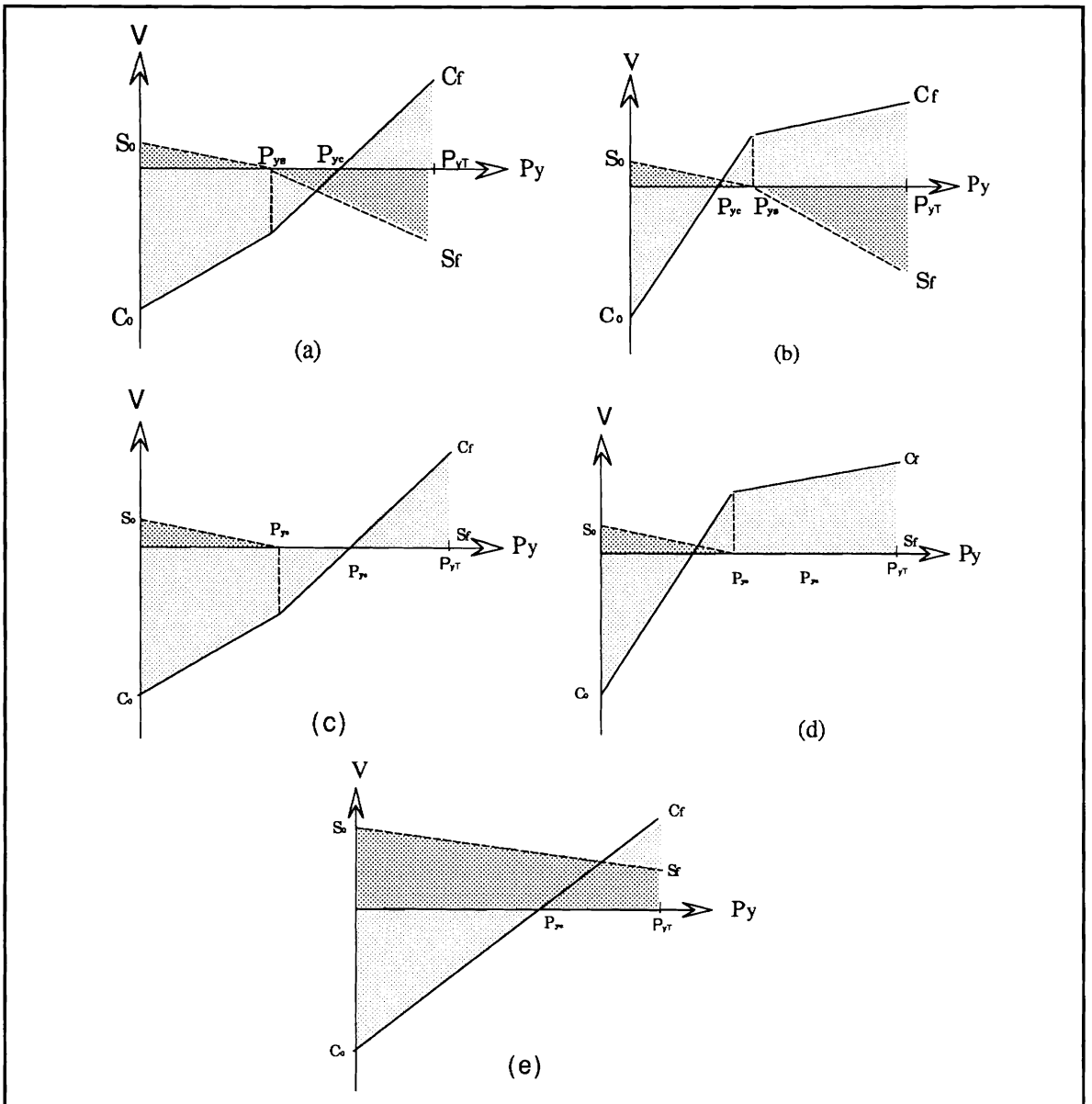

Figure 2 The Velocity-Impulse (V-P) Diagram for Impacts

Velocity-impulse (V-P) diagrams for the five cases are shown in Figure 2. In each case the relative velocity components are initially S_0 (tangential) and C_0 (normal). At the end of the impact, these velocities are S_f and C_f respectively. P_{yT} is the total normal impulse. P_{ys} is the impulse at which the relative tangential motion stops after which either a reversal of sliding (Cases (a),(b)) or sticking (Cases (c),(d)) can occur. P_{yc} is the value of impulse at which the relative normal velocity becomes zero and the compression phase ends. This is followed by the restitution phase. Any impact model should be capable of predicting P_{yT}, P_{yc} and P_{ys} whereupon, Equation (2.2) can be used to obtain the tangential component of impulse.

2.3 Impact Hypotheses

In this section we briefly discuss three different impact models that have been used by previous researchers. In the next subsection, we reject two such models on the grounds that they appear to violate energy conservation principles while a third model appears to be free of such problems.

Newton's Kinematic Hypothesis

Newton's law of impact states that the ratio of normal relative velocity at the contact point after impact to the same velocity before impact is equal to e, the coefficient of restitution. Therefore in the V-P diagram, the coefficient of restitution can be defined as

$$e = -\frac{C_f}{C_0} \tag{2.3}$$

Poisson's Impulse Hypothesis

A discussion of Poisson's hypothesis that can be found in [61,35]. It states that the impulse in the restitution period is e times that in the compression period. That is,

$$e = \frac{(P_{yT} - P_{yc})}{P_{yc}} \tag{2.4}$$

More recently, Wang and Mason [71] used Poisson's hypothesis and Routh's graphical technique to develop a systematic method for analyzing impact problems. The approach in Han and Gilmore [23] and Keller [34] is similar. The work in [34] is more general in the sense that it is applicable to three dimensional examples. Wang and Mason [71] advocate the principle of constraints [35] which allows for impulses if (and only if) it is not possible to satisfy constraints with finite forces. This in turn allows tangential impulses even in situations without impact. Although such impulses are not based on any physical laws, their use is attractive from a mathematical viewpoint since they offer a solution to anomalies that arise in rigid body mechanics, such as the inconsistency in the sliding rod problem.

Energy Hypothesis

Stronge [69] develops a new hypothesis for modeling frictional impacts which he calls the *internal dissipation energy* hypothesis. The coefficient of restitution is defined as the square root of the ratio of the energy released at the contact during restitution to the energy absorbed by deformation during compression. In this definition, the energy lost entirely represents only internal energy dissipation. If the tangential compliance of the contact is neglible, this is determined directly from the work done by the normal component of the impulse force.

In all these three models, it is possible to obtain analytical expressions for P_{yT}, P_{yc} and P_{ys} based on two parameters μ and e and the initial conditions S_0 and C_0. These expressions are complicated and therefore relegated to an appendix (Appendix 1). In each case, the energy dissipation during the collision can be calculated. It is the negative of the work done by the impulses,

$$D = -\int \mathbf{v} \bullet d\mathbf{P} \tag{2.5}$$

There is a fourth approach in the literature. Brach [8] treats impacts with tangential impulses in a somewhat different manner. The normal velocity components are determined through Newton's law using a hypothesized coefficient of restitution, while the tangential components are determined by frictional impulses. The ratio of tangential to normal impulses is such that it is less than

(a) the coefficient of dry friction (Coulomb's coefficient of friction)

(b) a critical value above which the tangential component of relative velocity is reversed

(c) a maximum value at which the energy loss is zero (for all values above this value, the energy loss is negative, and therefore inadmissible)

It can be shown that the energy hypothesis is the only model which ensures that the energy loss from sources other than friction is non-negative, and is zero when $e = 1$. This is demonstrated in Section 2.4 with the help of an example. Although the resulting analytical expressions are somewhat more complicated, this approach is most satisfying. A critical review of the first two hypotheses is also found in Reference [77].

2.4 Example

The classical example of a rigid rod contacting the ground (a rigid flat surface) as shown in Figure 3, is used in this paper. The rod's initial orientation is $\theta = 45$ degree, and the initial angular velocity is zero. The rod has unit mass and unit length. Note that $M_1=1$, moment of inertia $I_1 = \frac{1}{12}$, static friction coefficient $\mu_s = -0.6$. If the initial tangential velocity (S_0) is 0.6 and compressive velocity (C_0) is -1.0, then it can be shown that reversed sliding on

compression (Case (a)) occurs for $\mu < 0.6$ while sticking on compression (Case (c)) occurs for $\mu > 0.6$.

The solutions are shown in Figure 3 using Routh's graphical technique [61,71]. The arrows indicate the increase in normal and tangential impulses (from zero) during the collision process. Of course, the whole process occurs over a very short time interval. Since the bodies slide over each other at the beginning of impact, the impulse will develop along the *line of limiting friction, F*. This line satisfies the extension of Coulomb's law of impulse: $dP_x = \mu\, dP_y$. The impulse increases to the point at which the relative tangential velocity becomes zero (the point of intersection of *S* and *F*). If $\mu > 0.6$, the impulse increment will follow the *line of sticking, S*, this is the line when S=0. This is case (c). On the other hand, if $\mu < 0.6$, the increment will follow the dash line, the *line of reversed sliding, RF*. This is case (a). Line *C* represents C=0.

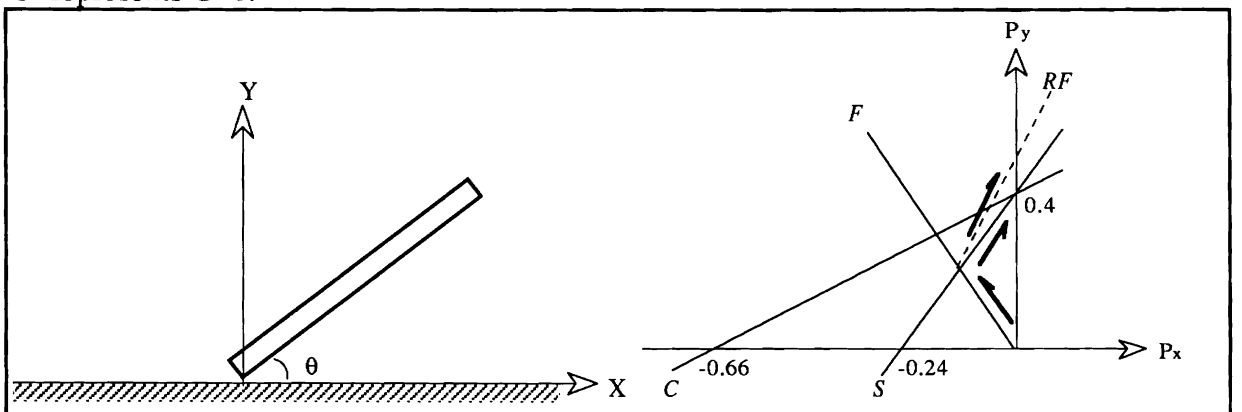

Figure 3 The Falling Rod Example

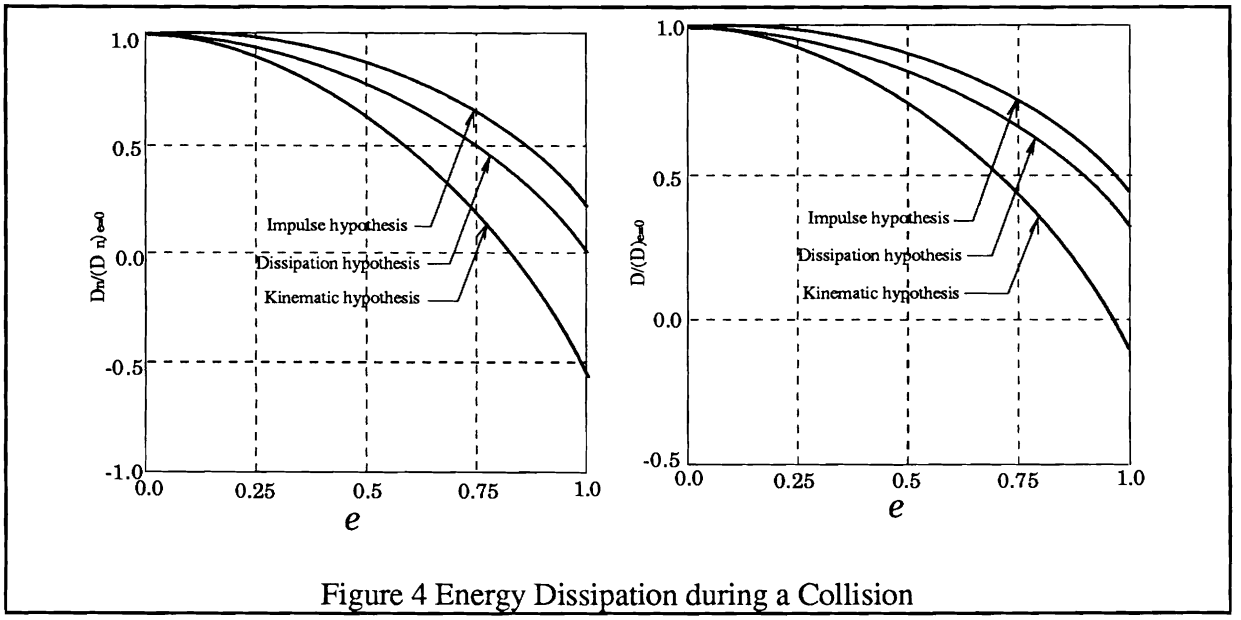

Figure 4 Energy Dissipation during a Collision

Consider, for example, Case (a), sliding and reverse sliding in compression phase. The dissipation energy is plotted with respect to the coefficient of restitution in Figure 4. D is the total dissipation energy while D_n is the dissipation calculated by using the normal velocity and impulse components only. In both plots the dissipation energy is normalized using the dissipation for the e=0 case. We can see that the kinematic hypothesis results in *negative dissipation* (that is, an energy gain) for large e. On the other hand, the impulse hypothesis predicts that the normal impulsive force does negative work even when e=1. In other words, when e=1, although D is nonnegative (as expected) $D_n>0$! Only Stronge's internal dissipation hypothesis results in a zero energy loss ($D=D_n=0$) when the coefficient of restitution e=1. This latter observation is not surprizing because the hypothesis *is* derived from energy dissipation considerations. Since Stronge's internal dissipation hypothesis does not violate the energy conservation law, it is preferable to the other two hypotheses. However it should be noted that it is only a hypothesis and is not derived from any law of physics.

3 Simulation with Rigid Body Models

3.1 Formulation

Consider a mechanical system with rigid bodies in a d-dimensional space (d = 3 for planar and 6 for spatial systems). Let $\mathbf{q}$ be the vector of n generalized coordinates for the system. The mechanical system can be described by a set of nonlinear coupled differential equations:

$$\mathbf{M}\,\ddot{\mathbf{q}} + \mathbf{c}(\mathbf{q}, \dot{\mathbf{q}}) = \mathbf{f} + \mathbf{G}\lambda \tag{3.1}$$

where $\mathbf{M}(\mathbf{q})$ is a symmetric, positive definite $n\times n$ inertia matrix with masses and moments of inertia of the different bodies, $\mathbf{c}$ is a $n\times 1$ vector including inertial forces that are nonlinear function of the velocities (for example, centrifugal and Corriolis forces), $\mathbf{f}$ is a $n\times 1$ vector of external forces, λ is the $k\times 1$ vector of multipliers or constraint forces, and $\mathbf{G}$ is a $n\times k$ Jacobian matrix whose columns represent the directions of the k constraints.

We assume, for convenience, that the holonomic (bilateral) constraints have been eliminated so that $\mathbf{q}$ represents a minimal set of generalized coordinates, such that $\mathbf{M}$ is nonsingular [28,54,60,72]. Of course if a larger set of coordinates is used, the constraint forces due to the bilateral constraints appear explicity as multipliers in (3.1). Since simulation of bilaterally constrained dynamic systems has been extensively studied [15,25,53,66], this subject is not discussed any further here. Finally, we restrict the treatment here to planar systems. The basic concepts are applicable to spatial systems although the level of complexity of the equations increases in a six dimensional space.

We allow for m unilateral constraints. The solution to (3.1) must satisfy the system of m unilateral (one-sided) constraints,

$$\Phi(\mathbf{q}) \geq 0 \tag{3.2}$$

where $\Phi = [\phi_1 \ \ \phi_2 \ \ldots \ \phi_m]^T$. In additional, there may be l non-integrable, nonholomic constraints that have one of the following two forms:

$$\kappa(\mathbf{q})\,\dot{\mathbf{q}} = 0 \tag{3.3}$$

$$\Psi(\mathbf{q})\,\dot{\mathbf{q}} \geq 0 \tag{3.4}$$

In this paper we assume that such constraints are absent and we focus on one-sided constraints as in Equation (3.2). Denote the set of active constraints by A. We assume that k of the m constraints in (3.2) are active.

Consider first the case of frictionless point contacts. If λ_i denotes the constraint force or the multiplier corresponding to ϕ_i,

$$\phi_i \geq 0,\ \lambda_i \geq 0,\ \phi_i\,\lambda_i = 0, \qquad i = 1,2,\ldots,m \tag{3.5}$$

The Jacobian matrix is determined by the k active constraints:

$$\mathbf{G} = [\mathbf{g}_1 \ \ \mathbf{g}_2 \ \cdots \ \mathbf{g}_k]$$

where

$$\mathbf{g}_i = \left[\frac{\partial \phi_i}{\partial q_1} \ \ \frac{\partial \phi_i}{\partial q_2} \ \cdots \ \frac{\partial \phi_i}{\partial q_k}\right]^T$$

In a simulation problem, the state ($\mathbf{q}$ and $\dot{\mathbf{q}}$) and external forces are given, and therefore in Equation (3.1), $\mathbf{c}$, $\mathbf{M}$, and $\mathbf{f}$ are known quantities. The objective is to find $\ddot{\mathbf{q}}$ and if possible, λ. It is convenient to lump the known vectors, $\mathbf{c}$ and $\mathbf{f}$, into a single vector $\mathbf{b}$ and rewrite (3.1):

$$\mathbf{M}\,\ddot{\mathbf{q}} = \mathbf{b} + \mathbf{G}\lambda,\ \lambda \geq 0 \tag{3.6}$$

If all the k constraints in A remain active and A remains unchanged through a finite time interval (that is, there are no transitions from "contact" to "no contact", or the other way around), the relative velocity ζ_i and the relative acceleration between the contacting bodies at the contact point vanishes.

$$\zeta_i = \mathbf{g}_i^T\,\dot{\mathbf{q}} = 0 \ \text{ and } \eta_i = \mathbf{g}_i^T\,\ddot{\mathbf{q}} + \dot{\mathbf{g}}_i^T\,\dot{\mathbf{q}} = 0 \tag{3.7}$$

or,

$$\eta = [\eta_1 \;\; \eta_2 \ldots \eta_m]^T = \mathbf{G}^T \ddot{\mathbf{q}} + \dot{\mathbf{G}}^T \dot{\mathbf{q}} = 0 \tag{3.8}$$

Substituting from (3.7), we get

$$\mathbf{G}^T \; (\mathbf{M}^{-1}[\, \mathbf{b} + \mathbf{G}\lambda \,]) \; + \; \dot{\mathbf{G}}^T \dot{\mathbf{q}} = 0 \tag{3.9}$$

If the constraints are linearly independent (which implies rank($\mathbf{G}$) = k < n), the constraint force vector, λ, can be obtained from (3.9) and $\ddot{\mathbf{q}}$ can be obtained by substituting for λ in (3.6). If they are linearly dependent, $\varpi = \mathbf{G}\lambda$ (n unknowns) can still be obtained by solving the k dependent equations in (3.8) [43], but λ cannot be determined uniquely. In this latter case, the system is statically indeterminate. Nevertheless, it is possible to substitute for $\mathbf{G}\lambda$ in (3.6) and solve for $\ddot{\mathbf{q}}$.

3.2 Changes in Topology

So far we assumed there are no changes in the constraints and the constraints are frictionless. We now proceed to relax these assumptions.

Active unilateral constraint becomes inactive

If a previously active constraint ϕ_i becomes inactive at time t_0, the corresponding constraint force λ_i must vanish. In other words,

$$\lambda_i \;\; \phi_i = 0 \tag{3.10}$$

Assume that all constraints are active from t = 0 to t=t_0. Since $\phi_i(\mathbf{q})>0$ at t_0, there must be small intervals Δt_1 and Δt_2 ($0 < \Delta t_1 < \Delta t_2$) such that

$$\zeta_i = 0 \text{ for } 0 < t \leq t_0 - \Delta t_1, \qquad \zeta_i > 0 \text{ for } t_0 - \Delta t_1 < t \leq t_0$$

$$\eta_i = 0 \text{ for } 0 < t \leq t_0 - \Delta t_2, \qquad \eta_i > 0 \text{ for } t_0 - \Delta t_2 < t \leq t_0$$

Differentiating (3.10) and recognizing that ϕ_i and ζ_i are zero in the interval $0 \leq t \leq t_0 - \Delta t_2$:

$$\lambda_i \;\; \zeta_i = 0, \qquad \lambda_i \;\; \eta_i = 0 \tag{3.11}$$

Therefore, in a finite time interval ($0 \leq t < t_0$), if no passive constraints become active, but we allow for the possibility of active constraints becoming passive at t_0, then for each of the k active constraints:

$$\lambda^T \eta = 0, \;\; \lambda \geq 0, \;\; \eta \geq 0, \quad \text{for } 0 \leq t \leq t_0 - \Delta t_2$$

Now, substitution of (3.6) yields:

$$\ddot{\mathbf{q}} = \mathbf{M}^{-1}[\mathbf{b} + \mathbf{G}\lambda]$$

$$\mathbf{G}^T\ (\mathbf{M}^{-1}[\ \mathbf{b} + \mathbf{G}\lambda\ ])\ +\ \dot{\mathbf{G}}^T\ \dot{\mathbf{q}} = \eta\ \geq 0$$

$$\lambda^T \eta\ = 0$$

$$\lambda \geq 0 \qquad (3.12)$$

Inactive unilateral constraint becomes active

Consider a constraint i which does not belong to A at time $t = 0$ ($\phi_i(t) > 0$), but at $t = t_0$, $\phi_i(t_0) = 0$. This event is usually accompanied by $\zeta_i(t_0) < 0$, in which case there is an impact and therefore a discontinuity in the velocities [24,74]. Let $t^- < t_0 < t^+$ such that $t^- \rightarrow t^+$, and let $\dot{\mathbf{q}}(t^-) = \dot{\mathbf{q}}^-$ and $\zeta_i(t^-)=\zeta_i^-$. Similarly, let $\dot{\mathbf{q}}(t^+) = \dot{\mathbf{q}}^+$, while $\zeta_i(t^+)=\zeta_i^+$. One approach is to use an appropriate impact model (as discussed in the previous section) to model the collision[2]. Impact models allow impulsive constraint forces and discontinuities in the velocities. Assuming that a satisfactory model for multiple contacts is available, we can determine $\dot{\mathbf{q}}^+$ from $\dot{\mathbf{q}}^-$. Although this is an approximate method, it is the only avenue of approach if rigid body models are used.

Frictional constraints

We use Coulomb's model for friction. We refer to the multipliers for the normal forces as λ_N and the frictional force multipliers as λ_F. The corresponding columns in the Jacobian, $\mathbf{G}$, are denoted by $\mathbf{g}_N$ and $\mathbf{g}_F$ respectively. Let the active constraint set of k constraints be divided into A_r (r rolling constraints, in which the relative tangential velocity at the contact point is zero), and A_s (s sliding contact constraints, in which the relative tangential velocity at the contact point is nonzero and the frictional force does nonzero work). The following conditions are evident for the $s+r$ frictional constraints:

$$\mu\lambda_{Ni} - |\lambda_{Fi}| \geq 0 \qquad (3.13a)$$

$$\zeta_{Fi}(\mu\lambda_{Ni} - |\lambda_{Fi}|) = 0 \qquad (3.13b)$$

$$\lambda_{Fi}\ \zeta_{Fi} \leq 0 \qquad (3.13c)$$

---

[2]Note that for a single contact, $\zeta_i^- = [C_0\ S_0]^T$ and $\zeta_i^+ = [C_f\ S_f]^T$.

where,

$$\zeta_{Fi} = \mathbf{g}_{Fi}^T \dot{\mathbf{q}} \text{ and } \zeta_{Ni} = \mathbf{g}_{Ni}^T \dot{\mathbf{q}}.$$

In addition, if $\zeta_{Fi} = \mathbf{g}_{Fi}^T \dot{\mathbf{q}} \neq 0$,

$$\lambda_{Fi} = \sigma_i \mu \lambda_{Ni}, \sigma_i = -sign(\zeta_{Fi})$$

else

$$\eta_{Fi} = \mathbf{g}_{Fi}^T \ddot{\mathbf{q}} + \dot{\mathbf{g}}_{Fi}^T \dot{\mathbf{q}}, \quad \eta_{Fi}(\mu\lambda_{Ni} - |\lambda_{Fi}|) = 0 \quad i = 1,2, ..., r+s \quad (3.13d)$$

In summary, simulation involves solving (3.12) for problems with frictionless constraints. For frictional contacts, (3.12) must be solved with the constraints in (3.13), but the formulation is similar. While there is no difficulty with solving (3.12) by itself, the constraints in (3.13) introduce problems. In the next subsection, we present an example which illustrates a potential problem with frictional contacts.

3.3 An Example with Inconsistencies

Consider the well known peg-in-the-hole insertion problem and a situation in which the axis of the peg and the axis of the hole are misaligned by a small angle of θ as shown in Figure 5. We assume that the hole has a chamfer (indicated by the angle α in the figure). This discussion is on the dynamic simulation while the example in Figure 1 considers only the two-point contact stage [73] .

A similar situation arises in the classical problem of a ladder (rod) being supported against a wall (Figure 6). Here the wall is inclined at an angle θ to the floor. Again we have a two point contact as in Figure 5 (although θ is shown much large in Figure 6). The free-body diagram is also shown in Figure 6. Here C is the midpoint of the rod (as also the midpoint of the segment AB in Figure 5), but not necessarily the center of mass of the rod or the peg. The external forces on the rigid body (including the velocity dependent inertial terms) are lumped together with the vector $\mathbf{b}$ (components b_x, b_y, and b_β). The motion of the rigid body is described by Equation (3.12), where $\mathbf{q} = [x \ y \ \beta]^T$. Let $\dot{\mathbf{q}}$ be such that two contacts are maintained and the angular velocity of the peg is clockwise, that is, $\dot{\beta} < 0$ (this is required if the peg must be assembled properly). Therefore, the frictional forces have the direction shown in Figure 6.

The Jacobian matrix is easily found from Figure 5 (or 6):

$\mathbf{g}_{N1} = \{0, 1, -(l \text{ Cos } \beta)\}^T$, $\mathbf{g}_{N2} = \{-\text{Sin } \theta, -\text{Cos } \theta, -(l \text{ Cos}[\beta+\theta])\}^T$

$\mathbf{g}_{F1} = \{1, 0, l \text{ Sin } \beta\}^T$, $\mathbf{g}_{F2} = \{-\text{Cos } \theta, \text{Sin } \theta, (l \text{ Sin}[\beta+\theta])\}^T$

Because the directions of the tangential velocities at the contact point are known (that is, ζ_{Fi}^+ and σ_i are known), **G** can be written as

$$\mathbf{G} = \left[\mathbf{g}_{N1}+\mu\sigma_1\mathbf{g}_{F1} \quad \mathbf{g}_{N2}+\mu\sigma_2\mathbf{g}_{F2}\right]$$

or,

$$\mathbf{G} = \begin{bmatrix} \mu & -\mu \text{ Cos } \theta - \text{ Sin } \theta \\ 1 & -\text{Cos } \theta + \mu \text{ Sin } \theta \\ -(l \text{ Cos } \beta - \mu l \text{ Sin } \beta) & -l \text{ Cos}(\beta+\theta) + \mu l \text{ Sin}(\beta+\theta) \end{bmatrix}$$

Substituting into the expression for η above, we have:

$$\eta = \mathbf{A}\,\lambda + \mathbf{e} \geq 0, \ \lambda \geq 0,$$

where,

$\lambda = [\lambda_1 \quad \lambda_2]^T$

$\mathbf{A} = \mathbf{G}^T\mathbf{M}^{-1}\mathbf{G}$

$$= \frac{1}{m}\begin{bmatrix} 1+\left(\frac{1}{k}\right)^2\left(\text{Cos}^2\beta - \mu \text{ Cos } \beta \text{ Sin } \beta\right) & \left(\frac{1}{k}\right)^2\left(-\mu \text{ Cos } \beta \text{ Sin}(\beta+\theta)\right) \\ -\text{Cos } \theta - \mu \text{ Sin } \theta + \left(\frac{1}{k}\right)^2 \text{Cos } \beta \text{ Cos}(\beta+\theta) & 1+\left(\frac{1}{k}\right)^2 \text{Cos}^2(\beta+\theta) \\ -\left(\frac{1}{k}\right)^2 \mu \text{ Sin } \beta \text{ Cos } (\beta+\theta) & -\mu\left(\frac{1}{k}\right)^2 \text{Cos } (\beta+\theta) \text{ Sin } (\beta+\theta) \end{bmatrix}$$

$$\mathbf{e} = \begin{bmatrix} \dfrac{b_y - \dfrac{l}{k^2} b_\beta \text{ Cos } \beta}{m} + l\,\dot{\beta}^2 \text{Sin } \beta \\ \dfrac{-\left(b_y \text{Cos } \theta + b_x \text{Sin } \theta\right) - \dfrac{l}{k^2} b_\beta \text{ Cos } (\beta+\theta)}{m} + l\,\dot{\beta}^2 \text{Sin } (\beta+\theta) \end{bmatrix}$$

Let $\mathbf{A} = \begin{bmatrix} a & c_1 \\ c_2 & d \end{bmatrix}$, while $\mathbf{e} = [e_1, e_2]^T$. We consider values of **f**, **M**, **q** and $\dot{\mathbf{q}}$, such that

1. $e_1, e_2 \leq 0$
2. $a, d \geq 0$
3. $c_1, c_2 \leq 0$
4. $|\mathbf{A}| \leq 0$

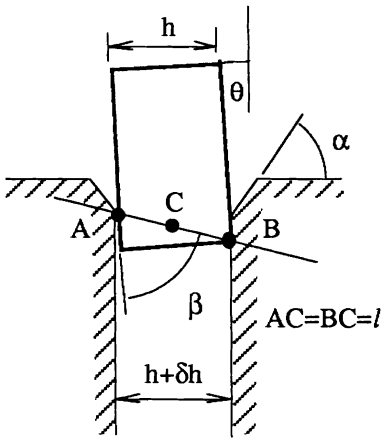

Figure 5

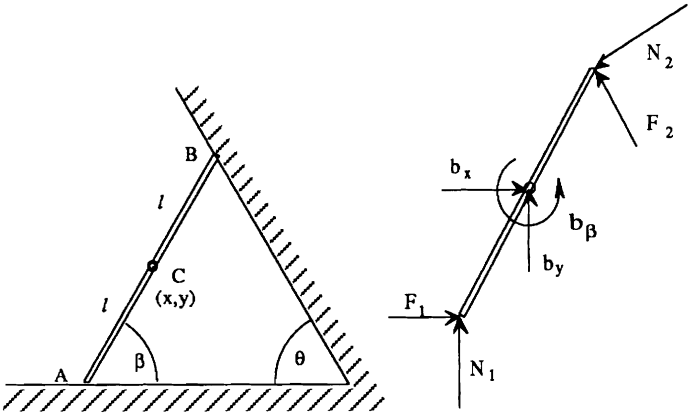

Figure 6

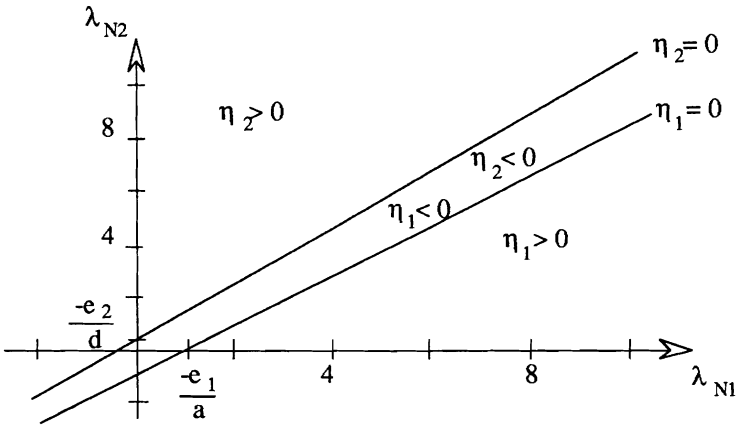

Figure 7

It is easy to see that it is always possible to satisfy condition 1 - for example, we let $b_\beta = 0$, $b_y < 0$, while b_x is sufficiently large and positive so that e_2 is zero. There is a entire range of parameters that satisfy conditions 2,3 and 4 too. For example, let m=1, k=1, $l = 1$ (with appropriate units) and $\mu = 0.4$, and consider a typical geometry, $\theta = 3$ degrees (which leads to $\beta = 73$ degrees for the example in Figure 5). For this situation, there is *no* λ_1 and λ_2 that yields a positive η_1 and η_2. This is shown in Figure 7. In fact, there is a entire range of θ and β for which these conditions are met and there are no solutions!

3.4 Discussion

The approach followed in Sections 3.1-3.3 is essentially the method adopted in most previous work on dynamic simulation of rigid body systems. Clearly, there are potential problems with such methods. Inconsistencies in rigid body analysis in problems with friction have been well known to Delassus, Klein, von Mises and Bouligand [7,43,47,52]. There are situations in which no solution for λ exist (as illustrated by the example in section 3.3), and others in which multiple solutions for $\ddot{\mathbf{q}}$ exist. More recently, Mason and Wang [47] and Featherstone [16] have also studied the inconsistencies in a rod sliding along a rough surface. Although the inconsistencies have been attributed to the approximate nature of Coulomb's law [47,52] and the inadequacy of rigid body models, no clear explanation has been found.

4 Contact Compliance

4.1 Background

Although rigid body models work very well for mechanical systems with bilateral constraints, they are not adequate for modeling contacts in systems with unilateral constraints. It is productive to model the compliance at each contact in such systems. The main benefit of this approach is that it allows small deformations at each contact and because of this, the problem of static indeterminacy is automatically resolved.

There are several approaches to modeling the contact compliance depending on the material properties and the geometry of the contacting surfaces. In this paper, we consider an example in which two elastic bodies come into contact. We make the realistic assumption that the contact deformations are small so that principles of linear elasticity are applicable. Further these deformations are small compared to the gross motion of the contacting bodies. For each contacting surface the geometry is mathematically modeled by a second order profile. The compliance at the contact is modeled by discretizing the contact area into small elements with lumped, linear stiffnesses. The numerical work by Kalker [31], Paul [55], Johnson [30] and many others [30] in solid mechanics is relevant here.

4.2 Method

The basic approach is to discretize the contact area into n_e small elements or contact patches with lumped stiffnesses. This is not unlike a finite element model. The inertial forces due to the deformation are small and are neglected. The contact area and deformations are

small compared to the gross dimensions of the contacting object. At the j^{th} contact patch for the i^{th} contact, the normal and tangential forces are N_{ij} and T_{ij} respectively. In other words,

$$\lambda_{Ni} = \sum_{j=1}^{n_e} N_{ij} \tag{4.1}$$

$$\lambda_{Fi} = \sum_{j=1}^{n_e} T_{ij} \tag{4.2}$$

The actual area of contact will be determined by the material properties and the geometry. Thus, the contact patches with nonzero forces will define this actual area.

Let δ_{in} denote the relative rigid body displacement in the normal direction at the *ith* contact as shown in Figure 8. Since the i^{th} constraint is ϕ_i, clearly $\delta_{in}= -\phi_i$. Let the profiles of the two contacting bodies (say 1 and 2) be given by $f^1(x)$ and $f^2(x)$. If $u^1_{in}(x)$ and $u^2_{in}(x)$ are the deformations for the two bodies, and $u_{in}(x_j) = u^1_{in}(x_j) + u^2_{in}(x_j)$,

$$u_{in}(x_j) - \delta_{in} + f^1(x_j) + f^2(x_j) = 0, \quad N_{ik} \neq 0 \qquad \text{inside the contact area}$$

$$u_{in}(x_j) - \delta_{in} + f^1(x_j) + f^2(x_j) \geq 0, \; N_{ik} = 0, \; T_{ik} = 0 \qquad \text{outside the contact area} \tag{4.3}$$

The displacement u^1_{in} (u^2_{in})is related to the pressure on body 1 (body 2) by the expression

$$u^1_{in}(x_j) = \sum_{k}^{n_e} [\xi^n_{jk} \; N_{ik} + \xi^t_{jk} \; T_{ik}] \tag{4.4}$$

where the *influence functions* ξ^n_{jk} and ξ^t_{jk} are the normal displacements at the contact patch j, due to a unit normal force and a unit tangential force at the contact patch k respectively. These influence functions are Green's functions [30,55] which depend on the contact geometry and the material properties.

Similarly, let δ_{it} denote the relative rigid body displacement in the tangential direction. If $u^1_{it}(x)$ and $u^2_{it}(x)$ are the tangential deformations for the two bodies, and $s_i(x)$ is the slip between the two contacting surfaces at x,

$$s_i(x_j) = s_{ij} = \delta_{it} - u^1_{it}(x_j) - u^2_{it}(x_j) \tag{4.5}$$

Of course, $s_i(x_j) = 0$ is indicative of no slip. If γ^n_{jk} and γ^t_{jk} are the tangential displacements at the contact patch j, due to a unit normal force and for a unit tangential force at the contact patch k respectively, the tangential displacement u^1_{it} (and similarly u^2_{it}) is given by:

$$u^1_{it}(x_j) = \sum_{k}^{n_e} [\gamma^n_{jk} \; N_{ik} + \gamma^t_{jk} \; T_{ik}] \tag{4.6}$$

If the contact is counterformal, that is the dimensions of the contact patch remain small compared to the radii of curvatures of the undeformed surfaces, it is appropriate to use elastic half space theory and influence functions derived by Boussinesq and Cerruti, which can be found in many standard texts in elasticity [45]. Similar functions have been derived for conformal contacts (where the above assumption is not valid) in Sternberg and Rosenthal

[68]. The point is analytical expressions for ξ^n_{jk}, ξ^t_{jk}, γ^n_{jk} and γ^t_{jk} are easily available (see for example, [30,55,66]).

Finally, the normal and tangential forces are subject to frictional constraints. The simplest constraint is generated by a point-wise application of Coulomb's (or Amonton's) law of friction:

$$\mu N_{ij} - |T_{ij}| \geq 0 \tag{4.7a}$$

$$s_{ij}\left(\mu N_{ij} - |T_{ij}|\right) = 0 \tag{4.7b}$$

$$T_{ij}\, s_{ij} \leq 0 \tag{4.7c}$$

Note that while this form of (4.7) is quite simple, it is possible to implement more complex models for friction. There are several aspects of frictional interaction between metallic bodies that suggest alternative *nonlinear* and *nonlocal* friction laws [50]. A nonlocal friction law predicts that motion (slip) will occur at a point of contact, when the shear stress at that point is equal to some function of the normal stress distribution in a neighborhood of that point. It is easy to implement such nonlocal laws in Equation (4.7).

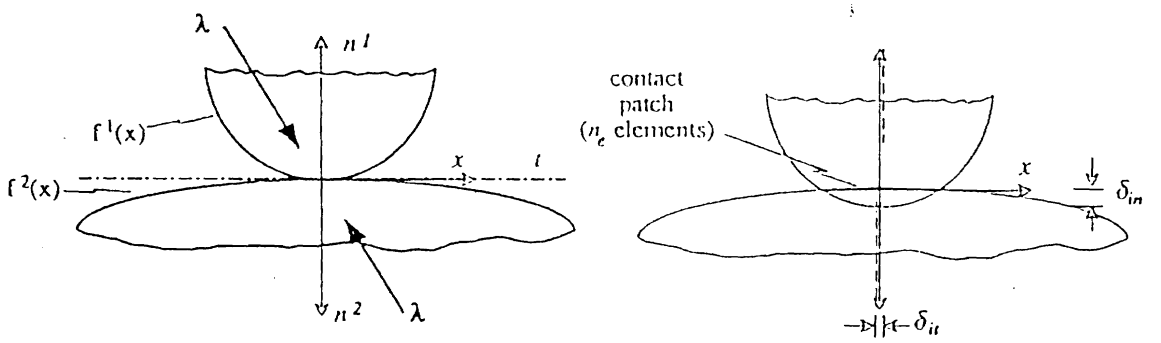

Figure 8

We proceed with the point-wise Coulomb's law in order to illustrate the method. Assume the rigid body relative motion (δ_{in} and δ_{it}) and the geometry is known. Equations (4.3-4) can be written for all the n_e contact patches at the *ith* contact in the form:

$$\mathbf{U}_i = \mathbf{A}_i\mathbf{N}_i + \mathbf{B}_i\mathbf{T}_i + \mathbf{C}_i$$

$$\mathbf{U}_i \geq 0$$

$$\mathbf{U}_i^T\, \mathbf{N}_i = 0$$

$$\mathbf{N}_i \geq 0 \tag{4.8}$$

where $\mathbf{U}_i$, $\mathbf{N}_i$ and $\mathbf{T}_i$ are $n_e \times 1$ vectors containing $u_{in}(x_j)$, N_{ij} and T_{ij} respectively, $\mathbf{A}_i$ and $\mathbf{B}_i$ are $n_e \times n_e$ matrices containing the influence coefficients while $\mathbf{C}_i$ consists of known constants

δ_{in}, δ_{it}, $f^1(x_j)$ and $f^2(x_j)$. Clearly, if there is no friction and $\mathbf{T} = 0$, this can be solved by considering a convex QP of the type:

$$\min_{N_i \geq 0} \quad \frac{1}{2} \mathbf{N}_i^T \mathbf{A} \mathbf{N}_i^T + \mathbf{N}_i^T \mathbf{C}_i \tag{4.9}$$

The objective function can be identified as the potential energy of the system and the minimization is the application of the minimum potential energy theorem [60,74].

However, the presence of friction introduces coupling between the normal and tangential components. Now, (4.8) must be solved for $\mathbf{N}_i$ and $\mathbf{T}_i$ along with the following equations:

$$\mathbf{S}_i = \mathbf{D}_i\mathbf{N}_i + \mathbf{E}_i\mathbf{T}_i + \mathbf{F}_i \tag{4.10a}$$

$$\mathbf{S}_i^T \mathbf{T}_i \leq 0 \tag{4.10b}$$

$$\mathbf{S}_i^T(T_i - \mu|N_i|) = 0 \tag{4.10c}$$

Equations (4.8) and (4.10) are equivalent to a nonlinear programming problem which can be solved using standard algorithms.

4.3 Example with Frictional, Elastic Contact

Consider the situation shown in Figure 3 with μ=0.4. We assume linear elastic properties and that the rod is rigid compared to the ground. The material properties of the ground (wall) are given by a modulus of elasticity of $3x10^6$ N/m^2 and a Poisson's ratio of 0.3. The contact surface of the rod is assumed to be cylindrical of radius 0.01 m, while the ground is flat. The positions and velocities before contact are exactly the same as in the example in Section 2 (Figure 3).

In Figure 9, the normalized deformations in the normal and tangential directions (x^* and y^*), the normalized velocities (C^* and S^*), the normalized contact force (λ_x^* and λ_y^*) and the normalized mechanical energy of the rod (D^*) are plotted against time (τ). τ is the nondimensionalized time parameter which is defined by

$$\tau = (t - t_0) / T$$

where T is the duration of the collision process (1.9 msec in this example), and t_0 is the instant at which contact first occurs. The normalizing variables for deformations, velocities and forces are the maximum normal deformation, initial velocity (C_i), the maximum normal contact force and initial mechanical energy, respectively. Results for the rigid body model (with the Energy hypothesis) and for the compliant contact model are shown in the figure for the e=1 case.

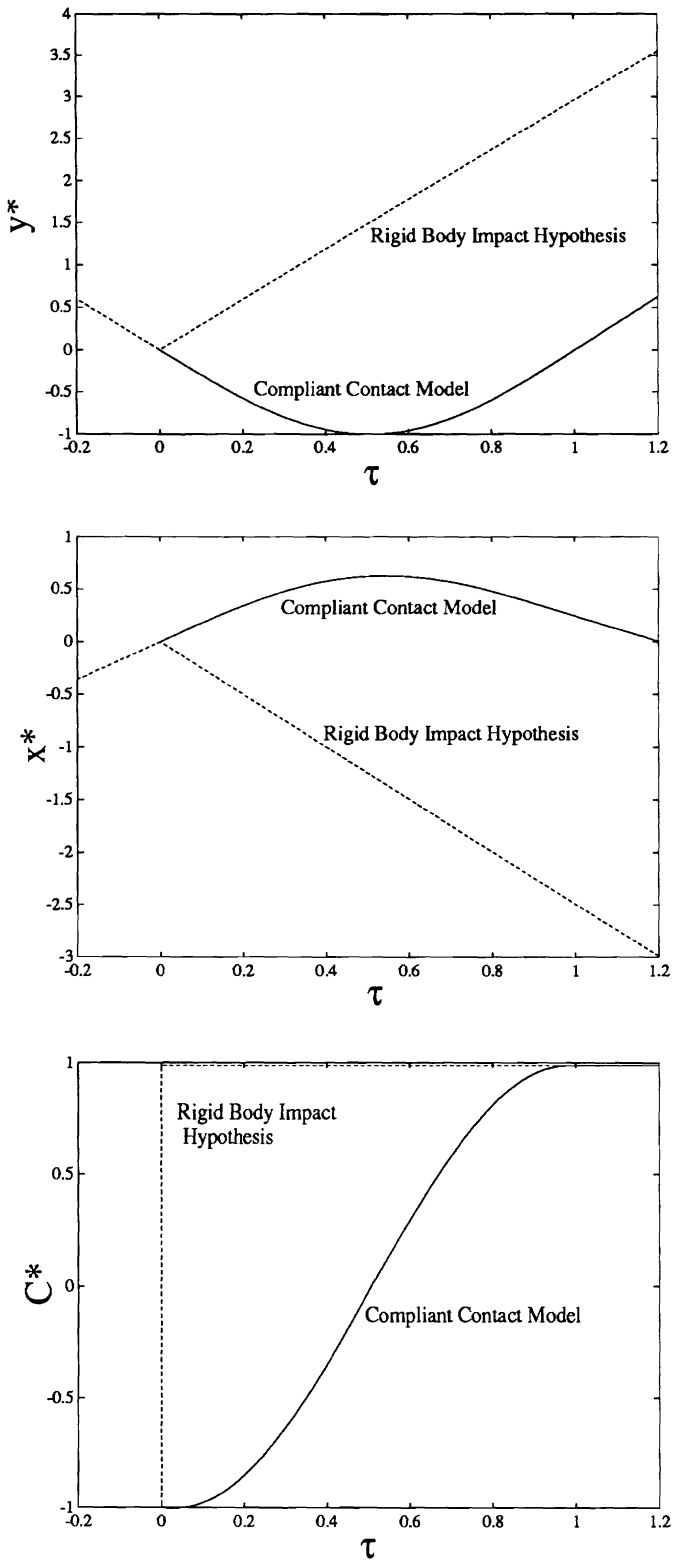

Figure 9 Simulation of an Impact using an Elastic Contact Stress Model

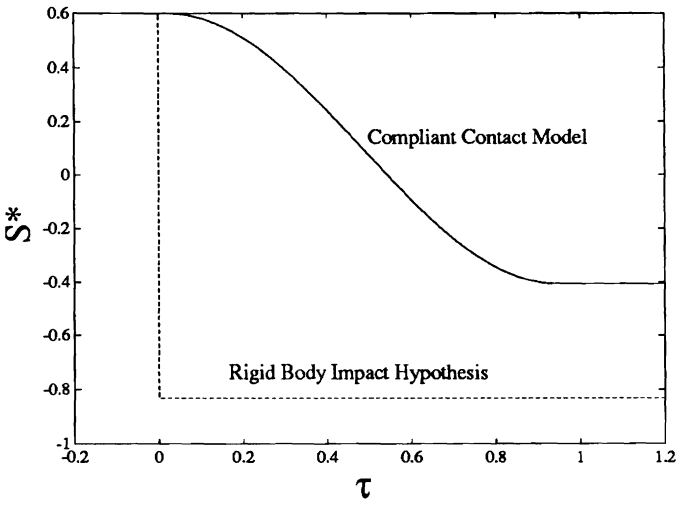

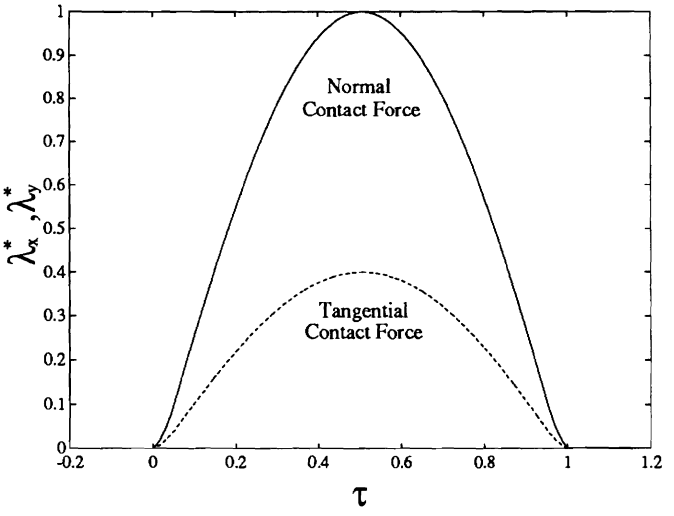

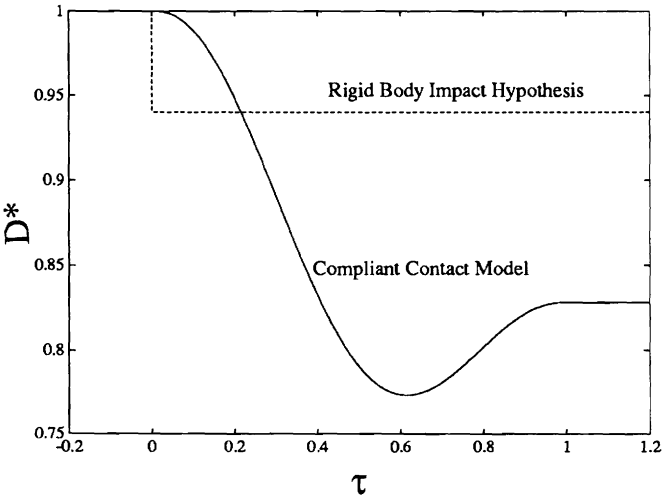

Figure 9 Simulation of an Impact using an Elastic Contact Stress Model (Continued)

Note that the compliant contact model predicts the contact forces, the deformations and the losses in energy. The two models are consistent only as far as the normal velocity is concerned. The contact force during the collision exhibits an impulsive behavior — it rises to 2700N (the weight is less than 10N). The compliant contact model predicts higher energy loss because of the friction compared to the rigid body model.

4.4 Example with Viscoelastic Contact

Once again, the example in Figure 3 is considered here. This time we examine the case where $\mu=0$ but the ground is a viscoelastic, rubber-like material. A Kelvin-Voigt model [30] is chosen for each contact patch. This model consists of a stiffness element and a dashpot in parallel. If the spring stiffness is k and the dashpot constant is c, the time constant, T_1 is given by:

$$T_1 = \frac{c}{k}$$

In Figure 10, results from a simulation are presented for the case $T_1=0.01$. This is compared with the results from Stronge's Energy hypothesis with $e=0.94$. Here e was chosen so that the energy dissipation is equal for the two modeling techniques. However this means that the two models will predict different separation velocities. This can be seen from the plots of y^* – the slopes of the two plots are different for $\tau>1$!

4.5 Discussion

Although this example was deliberately kept simple, this technique is powerful and quite general. It is more accurate because the strain energy is explicitly modeled and the phenomenon of micro-slip and frictional dissipation is incorporated. It is possible to model any contact geometry and any material by taking appropriate influence coefficients. For example, visco-elastic models can be used to incorporate a mechanism for energy dissipation. The method takes into consideration the dependence on the history of loading, and the fact that the displacement at any point on the contact surface depends on the traction and pressure through out the contact. It is also possible to accommodate any kind of *local* or *nonlocal* friction law by appropriately formulating the constraints. Finally, we note the uniqueness and existence of solutions to contact problems with friction have been dealt with in [14,50] and the problem of static indeterminacy is automatically resolved.

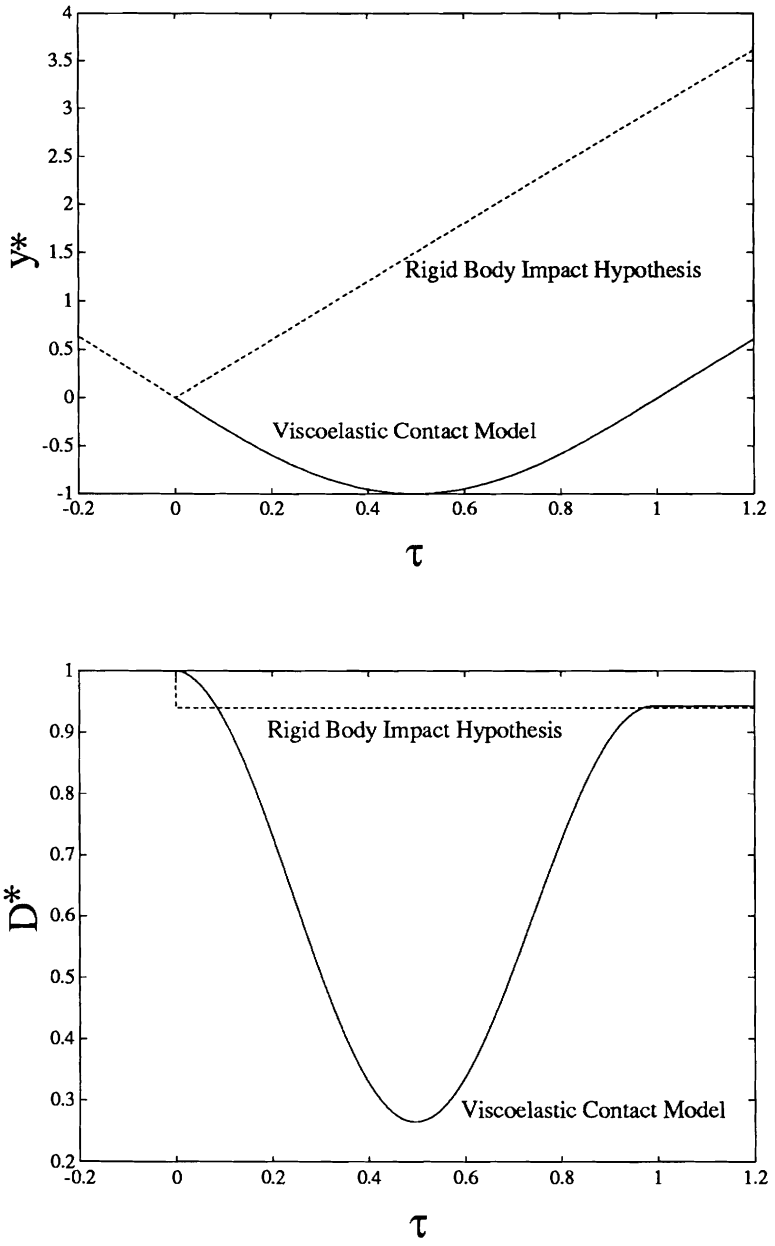

Figure 10 Simulation of an Impact using a Viscoelastic Contact Stress Model

5 Concluding Remarks

Rigid body models are inadequate for the dynamic analysis and simulation of processes with multiple, frictional contacts. In particular, two severe limitations are demonstrated in this paper: (a) The lack of a suitable model for collisions and impacts; (b) Incompatibility

with empirical frictional laws such as Coulomb's frictional law. A novel technique for the analysis for such problems is suggested in which rigid body models must be integrated with contact stress models. While the example chosen for this paper is relatively simple, it serves to illustrate the basic idea. The general method proposed in this paper has applications in a wide range of problems in manufacturing and robotics. Current work addresses the dynamic analysis of the peg-in-the-hole insertion process and simulation of nonlinear control algorithms for multiarm manipulation.

6 References

[1] G.Y. Andreev, and N.M. Laktionev. Problems in Assembly of Large Parts. *Russian Engineering Journal*, Vol. 46, No. 1, p. 40, 1966.

[2] G.Y. Andreev, and N.M. Laktionev. Contact Stresses During Automatic Assembly. *Russian Engineering Journal*, Vol. 49, No. 11, 1969.

[3] G.Y. Andreev. Assembling Cylindrical Press Fit Joints. *Russian Engineering Journal*, Vol. 52, No. 7, p. 54, 1972.

[4] N. I. Badler. Human factors simulation research at the University of Pennsylvania. *MS-CIS-90-67*. Department of Computer and Information Science. U. of Penn. Sept. 1990.

[5] D. Baraff. Analytical methods for dynamic simulation of non-penetrating rigid bodies. *Computer Graphics (Proc. SIGGRAPH)*. Vol. 23, 1988:223-232.

[6] B.M. Bazrov and A.I. Sorokin. The effect of clamping sequence on workpiece mounting accuracy. *Soviet Eng. Research.* 2(10):92-95, 1982.

[7] H. Béghin. Sur certain problémes de frottement. *Nouvelles Annales, 5e série* 2, pp. 305-312, 1923-24.

[8] R.M. Brach. Rigid body colisions. *ASME J. of Applied Mechanics.* Vol. 56. 1989: 133-138.

[9] R.W. Cottle and G.B. Dantzig. Complementary pivot theory of mathematical programming. *Lin. Alg. and Appl.*, 1, pp. 103-125, 1968.

[10] R.W. Cottle. *Numerical methods for complementarity problems in engineering and applied science*, computing Methods in Applied Sciences and Engineering. I. R. Glowinski and J.L. Lions, eds., Springer, Berlin, pp. 37-52, 1979.

[11] M. Cutkosky. Modeling and sensing finger/object contacts for automation and control. *Robotics Research.* Ed. K. Youcef-Toumi and H. Kazerooni.1989 (Presented at the 1989 ASME Winter Annual Meeting).

[12] B.R. Donald and D.K. Pai. On the motion of compliantly connected rigid bodies in contact: a system for analyzing designs for assembly. *IEEE Conf. on Robotics and Automation.* Cincinatti, OH, May 13-18, 1990: 1756-1762.

[13] W.S. Dorn. Duality in quadratic programming. *Quart. Appl. Math.*, 18, pp. 155-162, 1960.

[14] G. Duvaut and J.L. Lions. *Inequality in mechanics and physics.* Springer-Verlag, Berlin, 1976.

[15] A.G. Erdmann and D. Riley. New directions for mechanism kinematics and dynamics. *Computers in Mechanical Engineering.* Vol. 3, No. 6, 1985: 10-20.

[16] R. Featherstone. The dynamics of rigid body systems with multiple concurrent contacts. *Robotics Research: The Third International Symposium.* Eds., O.D. Faugeras and G. Giralt. MIT Press, 1986.

[17] J. Ferziger. *Numerical methods for engineering applications.* John Wiley and Sons. 1981.

[18] C.W. Gear. *Numerical Initial Value Problems in Ordinary Differential Equations*, Prentice-Hall, Englewood Cliffs, NJ, 1971.

[19] B. Gilmore. *The Simulation of Mechanical Systems with a Changing Topology.* Ph.D. thesis, Purdue University, Mechanical Engineering, August 1986.

[20] B.J. Gilmore and R.J. Cipra. Simulation of planar mechanical systems with changing topologies. *Proc. ASME Design Automation Conference*, 1987:369-388 (to appear in *ASME J. Mechanical Design*).

[21] D. Goldfarb and A. Idnani. A numerically stable dual method for solving strictly convex quadratic programs. *Mathematical Programming*. Vol. 27, 1983.

[22] A.S. Gusev. Automatic Assembly of Cylindrically Shaped Parts. *Russian Engineering Journal*, Vol. 49, No. 11, p. 53, 1969.

[23] I. Han and B.J. Gilmore. Multi-body impact motion with friction - analysis, simulation, and experimental validation. *Proc. ASME Design Technical Conferences*. Chicago, Sept. 16-19, 1990.

[24] E.J. Haug, S.C. Wu and S.M. Yang. Dynamics of mechanical systems with Coulomb friction stiction, impact and constraint addition-deletion-I. Theory. *Mech. Mach. Theory* 21, 401-406, 1986.

[25] M. Hiller and A. Kecskemethy. A computer-oriented approach for the automatic generation and solution of the equations of motion for complex mechanisms. *Proc. 7th World Congress on the Theory of Machines and Mechanisms*. Sevilla, 1987: 1135-1139.

[26] C.M. Hoffman and J.E. Hopcroft. Simulation of physical systems from geometric models. *IEEE Journal of Robotics and Automation*, RA-3(3): 194-206, June 1987.

[27] J. Hopcroft and G. Wilfong. Motion of Objects in Contact. *International Journal of Robotics Research*. Vol. 4 (4), 1986.

[28] R.L. Huston and C.E. Passerello. Eliminating singularities in governing equations of mechanical systems. *Mech. Res. Comm.*, 3, p. 361-365, 1976.

[29] A.W. Ingleton. A problem in linear inequalities. *Proc. London Math. Soc.* (3), 16, pp. 519-536, 1966.

[30] K.L. Johnson. *Contact Mechanics*. Cambridge University Press, London. 1985.

[31] J.J. Kalker. A survey of the mechanics of contact between solid bodies. *A. Angew. Math. Mech.*, 57, pp. T3-T17, 1977.

[32] S. Karamardian. The complementarity problem. *Math. Prog.*, 2, pp. 107-129, 1972.

[33] M.M. Karelin, and A.M. Girel. Accurate Alignment of Parts for Automatic Assembly. *Russian Engineering Journal*, Vol. 47, No. 9, p. 73, 1967.

[34] J.B. Keller. Impact with friction. *Journal of Applied Mechanics*, 53, pp. 1-4, 1986.

[35] C.W. Kilmister and J.E. Reeve. *Rational Mechanics*, Longmans, London, 1966.

[36] V. Kumar and K.J. Waldron. Force distribution in closed kinematic chains. *IEEE Journal of Robotics and Automation*, 4(6), December 1988.

[37] V. Kumar and J.H. Kim. A kinestatic analysis of cooperating robot systems. *5th International Conference on International Robotics*, Pisa, Italy, June 21-25 1991.

[38] V. Kumar, X. Yun, E. Paljug and N. Sarkar. Control of contact conditions for manipulation with multiple robotic systems. *IEEE Conference on Robotics and Automation*. Sacramento, April 7-12, 1991.

[39] N.M. Laktionev, and G.Y. Andreev. Automatic Assembly of Parts. *Russian Engineering Journal*, Vol. 46, No. 8, p. 40, 1966.

[40] H.M. Lankarani and P.E. Nikravesh. A contact force model with hysterisis damping for impact analysis of multibody systems. *Proc. ASME Design Automation Conference*. Vol. 2. 1989: 45-51.

[41] P. Lötstedt. *On a penalty function method for the simulation of mechanical systems subject to constraints*, TRITA-NA-7919, Dept. of Numerical Analysis and Computing Science, Royal Institute of Technology, Stockholm, 1979.

[42] P. Lötstedt. Coulomb friction in two-dimensional rigid body systems, *Zeitschrift für Angewandte Mathematik un Mechanik*. Vol. 61. No. 2:605-615, 1981.

[43] P. Lötstedt. Mechanical Systems of Rigid Bodies Subject to Unilateral Constraints. *SIAM J. Appl. Math.*, 42, pp. 281-296, 1982.

[44] P. Lötstedt. Numerical simulation of time-dependent contact and friction problems in rigid body mechanics. *SIAM Journal of Scientific and Statistical Computing*, 5(2): 370-393, 1984.

[45] A.I. Lur'e. *Three-dimensional problems of the theory of elasticity*. Interscience, New York. 1964 (English translation by J.R.M. Radok).

[46] M.T. Mason. Mechanics and Planning of Manipulator Pushing Operations. *International Journal of Robotics Research* 5(3), 1986.

[47] M.T. Mason and Y.Wang. On the inconsistency of rigid-body frictional planar mechanics. *IEEE Conference on Robotics and Automation*. Philadelphia, 1988:524-528.

[48] N.H. McClamroch. Singular systems of differential equations as dynamic models for constrained robot systems. *IEEE Conference on Robotics and Automation*. San Fransisco, pp. 21-28, 1986.

[49] K.G. Murty. *Linear complementarity, linear and nonlinear programming*. Heldermann Verlag, Berlin, 1988.

[50] J.T. Oden and E.B. Pires. Nonlocal and Nonlinear Friction Laws and Variational Principles for Contact Problems in Elasticity. *Journal of Applied Mechanics*. Vol. 50: 67-76, 1983.

[51] M.S. Ohwovoriole. *An Extension of Screw Theory and Its Application to the Automation of Industrial Assemblies*. Ph.D. thesis, Stanford University Department of Computer Science, Apr. 1980.

[52] P. Painlevé. Sur les lois du frottement de glissement. *C.R. Acad. Sci.*, 121, pp. 112-115; ibid. (1905), 140, pp. 702-707; ibid. (1905), 141, pp. 401-405 and pp. 546-552, 1895.

[53] B. Paul. Analytical dynamics of mechanisms - A computer oriented overview. *Mech. Mach. Theory*, 10, pp. 481-507, 1975.

[54] B. Paul. *Kinematics and dynamics of planar machinery*. Prentice Hall, Englewoods-Cliff, 1979.

[55] B. Paul and J. Hashemi. Contact Pressures on Closely Conforming Elastic Bodies. *Journal of Applied Mechanics*. Vol. 48:543-548, 1981.

[56] M. Peshkin. *Planning Robotic Manipulation Strategies for Sliding Objects*. Ph.D. thesis, Dept. of Physics, CMU, 1986.

[57] L. Petzold. Differential/Algebraic Equations are not ODEs, *this Journal*, 3, pp. 367-384, 1982.

[58] J.C. Platt and A.H. Barr. Constraint methods for flexible models. *Computer Graphics (Proc. SIGGRAPH)*. Vol. 22 (4), 1988:279-288.

[59] V.T. Rajan, R. Burridge, and J.T. Schwartz. Dynamics of a rigid body in frictional contact with rigid walls: motion in two dimensions. *Proceedings, 1987 IEEE Int. Conf. on Robotics and Automation*. Raleigh, North Carolina, 1987.

[60] R.M. Rosenberg. *Analytical dynamics of discrete systems.* Plenum Press, New York, 1977.

[61] E.J. Routh. *Dynamics of a system of rigid bodies.* MacMillan and co. London. 1891.

[62] K. Salisbury and B. Roth. Kinematics and force analysis of articulate mechanical hands. *ASME Journal of Mechanisms, Transmissions and Automation in Design,* 105:35-41, March 1983.

[63] V.M. Savischenko, and V.G. Bespalov. Orientation of Components for Automatic Assembly. *Russian Engineering Journal*, Vol. 45, No. 5, p. 50, 1965.

[64] K. Schittkowski. NLPQL: A FORTRAN subroutine solving constrained nonlinear programming problems. *Annals of Operations Research.* Vol. 5: 485-500, 1986.

[65] G.S.A. Shawki. Rigid considerations in fixture design. *Int. J. Mach. Tool Design and Res.* 7:195-209, 1967.

[66] P.N. Sheth and J.J. Uicker, Jr. IMP (Integrated Mechanisms Program), A computer-aided design and analysis system for mechanisms and linkage, Trans. ASME, Ser. B. J. Eng. Industr., 94, pp. 454-464, 1972.

[67] P.R. Sinha and J.M. Abel. A contact stress model for multifingered grasps of rough objects. *IEEE Int. Conf. on Robotics and Automation.* Cincinnati, OH, May 13-18, 1990:1040-1045.

[68] E. Sternberg and F. Rosenthal. The elastic sphere under concentrated loads. *ASME J. of Applied Mechanics.* Vol. 19, 1952, pp. 413-421.

[69] W.J. Stronge. Rigid body collisions with friction. *proceedings of the Royal Society of London*, A431, 168-181, 1990.

[70] R.H. Sturges. A Three-Dimensional Assembly Task Quantification with Application to Machine Dexterity. *Int. Journal of Robotics Research.* Vol. 7, No. 4, August 1988: 34-78.

[71] Y. Wang and M.T. Mason. Modeling impact dynamics for robotic operations. *Proceedings, 1987 IEEE Int. Conf. on robotics and Automation.* Raleigh, North Carolina, 1987.

[72] R.A. Wehage and E.J. Haug. Generalized coordinates partitioning for dimension reduction in analysis of constrained dynamic systems. *Journal of Mechanical Design.* Vol. 104. J1982:247-255.

[73] D.E. Whitney. Quasi-Static Assembly of Compliantly supported Rigid Parrs. *ASME J. Dynamic Systems, Measurement, and Control.* Vol. 104, 65:77, March 1982.

[74] E.T. Whittaker. *A Treatise on the Analytical Dynamics of Particles and Rigid Bodies*, 4th edition, Dover, New York.

[75] J. Wittenburg. *Dynamics of Systems of Rigid Bodies*, Teubner, Stuttgart, 1977.

[76] S.C. Wu, S.M. Yang and E.J. Haug. Dynamics of mechanical systems with Coulomb friction, stiction, impact and constraint addition-deletion-II. Planar systems. *Mech. Mach. Theory* 21, 407-416, 1986.

[77] Y. Wang and M.T. Mason. Two dimensional rigid body collisions with friction. *Journal of Applied Mechanics*, 1991 (to appear).

[78] X. Yun. Cooordination of Two-Arm Pushing. *IEEE Conference on Robotics and Automation.* 182-187, Sacramento, April, 1991.

Appendix 1: Analytical Expressions for Stronge's Energy Hypothesis

Consider the relative sliding velocity S(t) and the relative compression velocity C(t) of the contact point:

$$S = v_{1x} - v_{2x} = (\bar{v}_{1x}+r_{1y}\omega_1) - (\bar{v}_{2x}+r_{2y}\omega_2) = S_0 + \frac{P_x}{m_1} - \frac{P_y}{m_3} \quad \text{(A.1a)}$$

$$C = v_{1y} - v_{2y} = (\bar{v}_{1y}-r_{1x}\omega_1) - (\bar{v}_{2y}-r_{2x}\omega_2) = C_0 - \frac{P_x}{m_3} + \frac{P_y}{m_2} \quad \text{(A.1b)}$$

where

$$S_0 = S(t_0),\ C_0 = C(t_0),\ \frac{1}{m_1} = \frac{1}{M_1} + \frac{1}{M_2} + \frac{r_{1y}^2}{I_1} + \frac{r_{2y}^2}{I_2},$$

$$\frac{1}{m_2} = \frac{1}{M_1} + \frac{1}{M_2} + \frac{r_{1x}^2}{I_1} + \frac{r_{2x}^2}{I_2},\ \text{and}\ \frac{1}{m_3} = \frac{r_{1x}r_{1y}}{I_1} + \frac{r_{2x}r_{2y}}{I_2},$$

and k_1 and k_2 are the radius of gyration of object 1 and object 2, respectively. Note that the effective mass m_1, m_2 and m_3 are independent of velocity. If we assume forward sliding of the two bodies, the relation between the increment of tangential and normal impulse is

$$dP_x = - j\,\mu\, dP_y$$

where j is the direction of initial sliding velocity which is equal to $\frac{S_0}{|S_0|}$. Thus, Equation (A.1) can be written as

$$S = S_0 - P_y\left(\frac{j\,\mu\, m_3 + m_1}{m_1 m_3}\right) \quad \text{(A.2a)}$$

$$C = C_0 + P_y\left(\frac{j\,\mu\, m_2 + m_3}{m_2 m_3}\right) \quad \text{(A.2b)}$$

For impact case (a), sliding and reverse sliding in compression phase, the normal and tangential impulses can be determined by solving equation (A.1) with S=0 and C=0,

$$P_{ys} = \frac{m_1 m_3 S_0}{j\,\mu\, m_3 + m_1} \quad \text{(A.3)}$$

$$P_{yc} = \frac{m_2 m_3 C_0 + 2\, j\,\mu\, m_2 P_{ys}}{j\,\mu\, m_2 - m_3} \quad \text{(A.4)}$$

The dissipation for any period of slip is equal to the area between the line S or C and the abscissa, as shown in Figure 5. The dissipation due to the normal component of impact D_n

and that due to the tangential component of impulse D_t are found for impact case (a) by using Stronge's energy hypothesis:

$$D_n = -\frac{1}{2} C_0 P_{ys} - \frac{1}{2} C_0 P_{yT} + \frac{1}{2}\left(\frac{j\,\mu\, m_2 - m_3}{m_2\, m_3}\right)(P_{ys}\, P_{yc} + P_{yT}^2 - P_{yT} P_{yc})$$

$$- \frac{j\,\mu\, P_{ys}\, P_{yT}}{m_3} \qquad \text{(A.5a)}$$

$$D_t = \frac{1}{2} j\,\mu\, S_0 P_{ys} - \frac{1}{2}\, j\,\mu \left(\frac{j\,\mu\, m_3 - m_1}{m_1\, m_3}\right)(P_{yT} - P_{ys})^2 \qquad \text{(A.5b)}$$

The total dissipation $D = D_n + D_t$ and the total normal impulse, P_{yT}, is obtained as

$$e^2 = \frac{(P_{yT} - P_{yc})^2 \left(m_2\, m_3\, C_0 + (j\,\mu\, m_2 + m_3) P_{ys}\right)}{- m_2\, m_3\, C_0\, (P_{yc} - P_{ys})^2 - (j\,\mu\, m_2 + m_3) P_{ys}\, P_{yc}\, (P_{yc} - P_{ys})}$$

$$P_{yT} = P_{yc} +$$

$$e\left[\frac{C_0\, m_2\, m_3\, (P_{ys}^{\,2} - P_{yc}^2) + (j\,\mu\, m_2 + m_3)\, m_2\, m_3\, P_{ys}\, P_{yc}\, (P_{ys} - P_{yc})}{m_2\, m_3\, C_0 + (j\,\mu\, m_2 + m_3)\, P_{ys}}\right]^{\frac{1}{2}}$$

(A.6)